Sedimentation and Fouling of Optical Surfaces at the ANTARES Site

The ANTARES Collaboration

P. Amram [p], M. Anghinolfi [h], S. Anvar [d], F.E. Ardellier-Desages [d], E. Aslanides [b], J-J. Aubert [b], R. Azoulay [d], D. Bailey [s], S. Basa [b], M. Battaglieri [h], R. Bellotti [e], J. Beltramelli [d], Y. Benhammou [j], R. Berthier [d], V. Bertin [b], M. Billault [b], R. Blaes [j], R.W. Bland [d], F. Blondeau [d], N. de Botton [d,s], J. Boulesteix [p], C.B. Brooks [s], J. Brunner [b], F. Cafagna [e], A. Calzas [b], A. Capone [i], L. Caponetto [g], C. Cârloganu [q], E. Carmona [k], J. Carr [b], S.L. Cartwright [t], S. Cecchini [f,r], F. Ciacio [e], M. Circella [e], C. Compère [ℓ], S. Cooper [s], P. Coyle [b], S. Cuneo [h], M. Danilov [o], R. van Dantzig [q], C. De Marzo [e], J-J. Destelle [b], R. De Vita [h], G. Dispau [d], F. Druillole [d], J. Engelen [q], F. Feinstein [b], C. Ferdi [j], D. Festy [ℓ], J. Fopma [s], J-M. Gallone [n], G. Giacomelli [f], P. Goret [d], J-F. Gournay [d], G. Hallewell [b], A. Heijboer [q], J.J. Hernández-Rey [k], J. R. Hubbard [d], M. Jaquet [b], M. de Jong [q], M. Karolak [d], P. Keller [b], P. Kooijman [q], A. Kouchner [d], V.A. Kudryavtsev [t], H. Lafoux [d], P. Lagier [b], P. Lamare [d], J-C. Languillat [d], L. Laubier [a], J-P. Laugier [d], B. Leilde [ℓ], H. Le Provost [d], A. Le Van Suu [b], L. Lo Nigro [g], D. Lo Presti [g], S. Loucatos [d], F. Louis [d], V. Lyashuk [o], P. Magnier [d], M. Marcelin [p], A. Margiotta [f], R. Masullo [i], F. Mazéas [ℓ], B. Mazeau [d], A. Mazure [p], J.E. McMillan [t], E. Migneco [m], C. Millot [a], P. Mols [d], F. Montanet [b], T. Montaruli [e], L. Moscoso [d], M. Musumeci [m], E. Nezri [b], G.J. Nooren [q], J.E.J. Oberski [q], C. Olivetto [b], A. Oppelt-Pohl [b], N. Palanque-Delabrouille [d,*], R. Papaleo [m], P. Payre [b], P. Perrin [d], M. Petruccetti [i], C. Petta [g], P. Piattelli [m], J. Poinsignon [d,s], R. Potheau [b], Y. Queinec [d], C. Racca [n], G. Raia [m], N. Randazzo [g], F. Rethore [b], G. Riccobene [m], J-S Ricol [b], M. Ripani [h], V. Roca-Blay [k], A. Romeyer [d], A. Rostovstev [o], G.V. Russo [g], Y. Sacquin [d], E. Salusti [i], J-P. Schuller [d], W. Schuster [s], J-P. Soirat [d], O. Souvorova [j], N.J.C. Spooner [t], M. Spurio [f], T. Stolarczyk [d], D. Stubert [j], M. Taiuti [h], C. Tao [b], L.F. Thompson [t], S. Tilav [s], R. Triay [c], A. Usik [o], P. Valdy [ℓ], V. Valente [i], I. Varlamov [o], G. Vaudaine [k], P. Vernin [d], E. Vladimirsky [o], M. Vorobiev [o], P. de Witt Huberts [q], E. de Wolf [q], V. Zakharov [o], S. Zavatarelli [h], J. de D. Zornoza [k], J. Zúñiga [k]

and the CEFREM

J.-C. Aloïsi [u], Ph. Kerhervé [u], A. Monaco [u]

[a] *COM – Centre d'Océanologie de Marseille, CNRS/INSU Université de la Méditerranée Aix-Marseille II, Station Marine d'Endoume-Luminy, Rue de la Batterie des Lions, 13007 Marseille, France*

Preprint to be submitted to Astroparticle Physics *15 January 2003*

[b] *CPPM – Centre de Physique des Particules de Marseille, CNRS/IN2P3 Université de la Méditerranée Aix-Marseille II, 163 Avenue de Luminy, Case 907, 13288 Marseille Cedex 9, France*

[c] *CPT – Centre de Physique Théorique, CNRS, 163 Avenue de Luminy, Case 907, 13288 Marseille Cedex 09, France*

[d] *DSM/DAPNIA, CEA/Saclay, 91191 Gif Sur Yvette Cedex, France*

[e] *Dipartimento Interateneo di Fisica e Sezione INFN, Via E. Orabona 4, 70126 Bari, Italy*

[f] *Dipartimento di Fisica dell'Università e Sezione INFN, Viale Berti Pichat 6/2, 40127 Bologna, Italy*

[g] *Dipartimento di Fisica ed Astronomia dell'Università e Sezione INFN, 57 Corso Italia, 95129 Catania, Italy*

[h] *Dipartimento di Fisica dell'Università e Sezione INFN, Via Dodecaneso 33, 16146 Genova, Italy*

[i] *Dipartimento di Fisica dell'Università "La Sapienza" e Sezione INFN, P.le Aldo Moro 2, 00185 Roma, Italy*

[j] *GRPHE – Groupe de Recherches en Physique des Hautes Energies, Université de Haute Alsace, 61 Rue Albert Camus, 68093 Mulhouse Cedex, France*

[k] *IFIC – Instituto de Física Corpuscular, Edificios Investigación de Paterna, CSIC – Universitat de València, Apdo. de Correos 22085, 46071 Valencia, Spain*

[ℓ] *IFREMER – Centre de Toulon/La Seyne Sur Mer, Port Brégaillon, Chemin Jean-Marie Fritz, 83500 La Seyne Sur Mer, France and IFREMER – Centre de Brest, BP 70, 29280 Plouzané, France*

[m] *INFN – Labaratori Nazionali del Sud (LNS), Via S. Sofia 44, 95123 Catania, Italy*

[n] *IReS – Institut de Recherches Subatomiques (CNRS/IN2P3), Université Louis Pasteur, BP 28, 67037 Strasbourg Cedex 2, France*

[o] *ITEP – Institute for Theoretical and Experimental Physics, B. Cheremushkinskaya 25, 117259 Moscow, Russia*

[p] *LAM – Laboratoire d'Astronophysique de Marseille, CNRS/INSU - Université de Provence Aix-Marseille I, Traverse du Siphon – Les Trois Lucs, BP 8, 13012 Marseille Cedex 12, France*

[q] *NIKHEF, Kruislaan 409, 1009 SJ Amsterdam, The Netherlands*

[r] *TESRE/CNR, 40129 Bologna, Italy*

[s] *University of Oxford, Department of Physics, Nuclear and Astrophysics Laboratory, Keble Road, Oxford OX1 3RH, United Kingdom*

[t] *University of Sheffield, Department of Physics and Astronomy, Hicks Building, Hounsfield Road, Sheffield S3 7RH, United Kingdom*

[u] *CEFREM – Centre de Formation et de Recherche sur l'Environnement Marin, Université de Perpignan, 66860 Perpignan, France*

Abstract

ANTARES is a project leading towards the construction and deployment of a neutrino telescope in the deep Mediterranean Sea. The telescope will use an array of photomultiplier tubes to detect the Cherenkov light emitted by muons resulting from the interaction with matter of high energy neutrinos. In the vicinity of the deployment site the ANTARES collaboration has performed a series of in-situ measurements to study the change in light transmission through glass surfaces during immersions of several months. The average loss of light transmission is estimated to be only $\sim 2\%$ at the equator of a glass sphere one year after deployment. It decreases with increasing zenith angle, and tends to saturate with time. The transmission loss, therefore, is expected to remain small for the several year lifetime of the ANTARES detector whose optical modules are oriented downwards. The measurements were complemented by the analysis of the ^{210}Pb activity profile in sediment cores and the study of biofouling on glass plates. Despite a significant sedimentation rate at the site, in the $0.02 - 0.05\,\mathrm{cm \cdot yr^{-1}}$ range, the sediments adhere loosely to the glass surfaces and can be washed off by water currents. Further, fouling by deposits of light-absorbing particulates is only significant for surfaces facing upwards.

Key words: Neutrino telescope; Undersea Cherenkov detectors; Sea water properties: fouling, sedimentation.
PACS: 07.89.+b, 29.40.Ka, 92.10.Bf, 92.10.Pt, 92.10.Wa, 95.55.Vj

* Corresponding author: Nathalie.Palanque-Delabrouille@cea.fr

1 Introduction

The ANTARES undersea neutrino telescope [1,2] will be dedicated to the detection of high energy neutrinos. The scientific programme covers searches for astrophysical, cosmological and dark matter neutrino sources, as well as the study of flavour oscillations for atmospheric neutrinos.
The selection of a suitable site for the telescope takes into account several parameters. The distance to shore dictates the length of the electro-optical cable needed to power the detector and transmit the data. The depth determines the rate of background from down-going cosmic ray muons, as well as the limiting angle of observation near the horizon. The nature and topography of the sea floor are relevant for the anchoring of the detector elements. Deep sea currents affect the geometry of the mooring lines comprising the detector. Meteorological conditions at the sea surface are critical for deployment and recovery operations. The optical background resulting from ^{40}K decay and bioluminescence [3] will affect trigger rates and track reconstruction, while bioluminescence bursts can induce dead-time in the data acquisition. The parameters which govern the transmission of Cherenkov light through the sea water to the optical modules are most important for the design and the performance of the detector; light absorption largely determines the total number of optical modules required for efficient detection, while light scattering mainly limits the angular resolution of the telescope. Given the objective of operating the telescope for several years without maintenance, it is mandatory that the active optical surfaces not be significantly fouled during this period.

This paper reports on a study of optical fouling in the vicinity of the ANTARES site (42°50′N 6°10′E), which is located 20 nautical miles (37 km) from Toulon at a depth of 2400 m. Direct measurements have been made of the change in light transmission through glass surfaces during immersions of several months. In order to extrapolate to longer periods of time, it is important to understand the nature of the fouling, particularly biofouling and sedimentation. Therefore measurements of light transmission were complemented by studies of biofouling on glass plates and by a detailed study of sedimentation. Different approaches were used to classify and quantify the particle sedimentation; total mass fluxes were determined by a time-series collection of samples in a sediment trap, particle concentration was measured in water samples taken at various depths, and sedimentation rates were calculated from the ^{210}Pb activity in a sea floor core sample.

2 Fouling and sedimentation measurement methods

Some of the measurements reported here were made using instruments on a recoverable mooring line, while others were made on samples obtained with the IFREMER deep sea manned submersible Nautile [4].

2.1 Mooring line

The mooring line is anchored to the sea bed by a sinker (dead weight) and held vertical by the flotation of buoys. The line is recovered by the remote activation of an acoustic release that disconnects it from the sinker. Figure 1

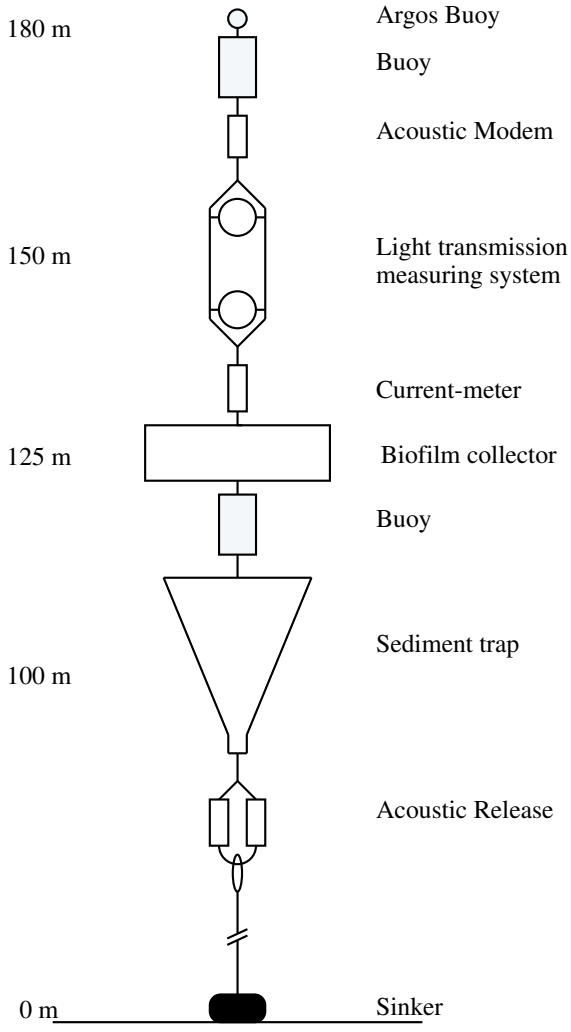

Fig. 1. The mooring line (figure not to scale), as configured for the first immersion. The light transmission measuring system was mounted horizontally for the second immersion.

is a sketch of the mooring line including information on approximate heights from the sea floor. The line is equipped with the following measuring systems (from top to bottom): a device measuring light transmission between two glass spheres, a mechanical current-meter [1], a biofilm collection system, and a sediment trap. These devices are described in the following sections.

The mooring line was immersed twice at a site (42°49′N 6°10′50″E) located approximately 1 nautical mile of the final site where the ANTARES detector is to be deployed. The first immersion lasted three months in 1997 and the second, eight months covering part of 1997 and of 1998.

2.2 The light transmission measurement system

The system for measuring light transmission, shown in figure 2, is housed in two 17″ pressure resistant glass spheres similar to those that will house the photomultiplier tubes (PMT) of the ANTARES detector. They are mounted on a support frame with their centres separated by 2.5 m.

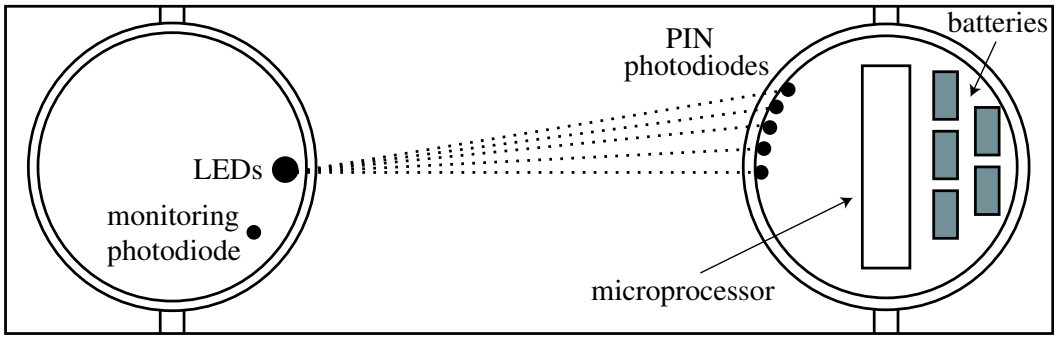

Fig. 2. The light transmission measuring system, showing the configuration used for the second immersion.

The first sphere holds a light source composed of two blue light emitting diodes [2] (LED). Each LED is monitored by a 5 mm^2 PIN photodetector [3] consisting of a photodiode with an operational amplifier. The two-LED system is designed to ensure the stability of the light source. All of these components are mounted on a holder glued to the inner surface of the glass sphere. The distance from the LEDs to the glass is 4 cm; the size of the illuminated area of the glass is 1 cm in diameter. A small mirror on the back of each LED collects the light emitted at large angles and focuses it on the active area of the monitoring photodiode.

[1] MC360 from MORS, www.mors.fr/products/currentmeter/index.html
[2] NSPB500 from NICHIA, www.nichia.co.jp
[3] OSI5 hybrid PIN photodetector from Centronic, www.centronic.co.uk

The second glass sphere contains five photodetectors glued to the inner surface of the sphere at various positions. Each photodetector consists of a silicon photodiode with a sensitive area of 1 cm^2 and an integrated amplifier. The light flux transmitted to each photodiode is measured in order to monitor the effect of fouling on the two glass surfaces, in front of the light source and in front of the photodiode.

The detector sphere contains the data acquisition board with the microprocessor and batteries to power the system. The microprocessor controls the measurement sequence and stores the digitised data (the output voltages from the photodiodes). An acoustic modem allows transmission of the data to the sea surface for regular verification of the detector status and for intermediate data transfers.

Light transmission measurements were performed twice a day at 0:00 and at 12:00 UT. For each photodiode, measurements of the dark current and the current produced under illumination with each of the two LEDs, were made in a programmed sequence. Each recorded measurement was the average of 10 readings. The entire sequence lasted 3 minutes.

For the first immersion (deployment January 25, 1997; recovery April 21, 1997), the support frame was vertical (as shown in figure 1) with the light source on top shining light vertically down to the detector sphere. Photodetectors were glued to the lower sphere at zenith angles (θ) of 0°, 20° and 40°. Three photodetectors were placed at 20° on different meridians to test for a possible azimuthal (ϕ) dependence of the fouling.

For the second immersion (deployment July 12, 1997; recovery March 12, 1998), the support frame was horizontal and the photodetectors were placed at zenith angles ranging from 50° to 90° on a single meridian facing the light source, as indicated in figure 2. During this immersion, for an unknown reason, the data acquisition stopped on January 31, 1998 and resumed on February 20, 1998.

2.3 The biofilm collection system

The biofilm collection system consists of a 1.2 m long horizontal rod supporting 12 cylindrical sample holders. Six 2.6×3.8 cm^2 glass plates are mounted on each sample holder as shown in figure 3.

During the descent of the mooring line, a cover protects the samples. A magnesium anode release system triggers the opening of the cover after a few hours of immersion. At the end of the exposure, an externally controlled acoustic release system actuates the closing of the cover in order to protect the glass

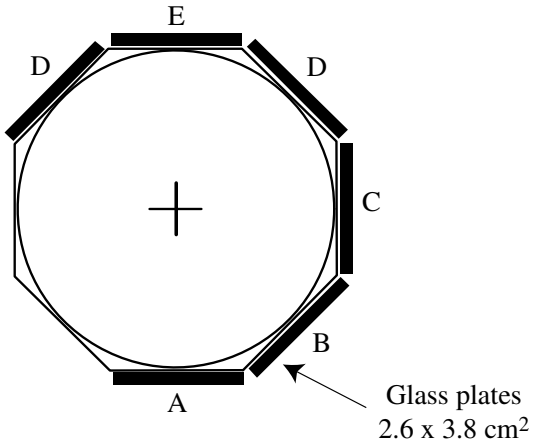

Fig. 3. Side view of a biofilm sample holder.

plates during the ascent of the line. After recovery, all glass slides are immersed in either a glutaraldehyde or a formaldehyde solution which fixes the biofilm. They were observed with a scanning electron microscope or stained with a fluorescent molecule in order to count the total number of bacteria by epifluorescence microscopy.

2.4 The sediment trap

A time-series sediment trap[4] mounted about 100 m above the bottom of the mooring line collected particles drifting towards the bottom. The trap (2.3 m high and 1.13 m in diameter) has a 1 m^2 collection area and a baffled conical design (36° opening angle). The baffle funnels the sediments into a series of 24 Teflon receiving cups, each having a volume of 250 ml. The trap was programmed to collect sediments on a weekly basis for the first 24 weeks after the immersion (from July 14 to December 29, 1997).

A complete description of the sample processing is given in [5]. Briefly, the receiving cups are filled before deployment with a buffered 5% formaldehyde solution in filtered sea water (0.45 μm) to limit in-situ microbial degradation and to reduce contamination by swimmers (organisms entering the trap actively, thus introducing an active component in addition to the passive settling flux). After recovery, the cups are stored in the dark at 2–4°C until processed. The most important step of the laboratory processing is the removal of the bulk of swimmers. Finally the remaining samples are de-salted and dried (40°C) for estimation of mass fluxes and other analyses.

[4] Sediment trap PPS5/2 from Technicap, www.technicap.com

2.5 Collection of core samples and water samples

The Nautile submarine, in the period from December 21 to December 24 1998, collected 6 sediment core samples from the sea floor and 4 water samples at various depths at the ANTARES site. To collect each core, a 10-centimetre diameter 40-centimetre long PVC pipe was thrust into the sea floor using the manipulator of the Nautile. The water samples were collected using plastic Niskin bottles which were initially held open, then closed using the Nautile manipulator at different heights from the sea bottom during the ascent of the submersible. The cores and the water samples were kept refrigerated until processed.

3 Data analysis

3.1 Light transmission measurements

The variation with time of the photodiode current, corrected for the dark current contribution, yields the evolution of the light transmission. Since the current depends on the photodiode position and sensitivity, the relevant quantity is the variation relative to the value measured immediately after immersion. For each photodiode we have checked that these relative variations did not depend (within $\pm$ 1% during the first immersion and $\pm$ 0.5% during the second immersion) on which of the two LEDs was used. Therefore the average of the measurements obtained for each of the two LEDs was used in the analysis. The resulting relative transmissions as a function of time are shown in figures 4 and 5 for the first and second immersion, respectively.

For both immersions the photodiodes located inside the light source sphere gave very stable readings, showing that the light intensity from the LEDs was constant to better than $\pm$ 0.2% throughout each of the two measurement periods.

Figures 4 and 5 show a general trend of decreasing fouling with increasing zenith angle on the glass sphere. In figure 4, we observe a very rapid decrease (within a few days) in the transmission at the top of the sphere ($\theta = 0°$), but less change at larger zenith angles. The transmission is seen to recover from time to time in partial correlation with an increase in the measured water current velocity (bottom of figure 4). These observations are consistent with the surfaces being fouled by sediments (rather than microbial adhesion and growth, see section 3.4) which are more likely to stay on horizontal surfaces than on inclined ones, and can be washed off by flowing water. The differences

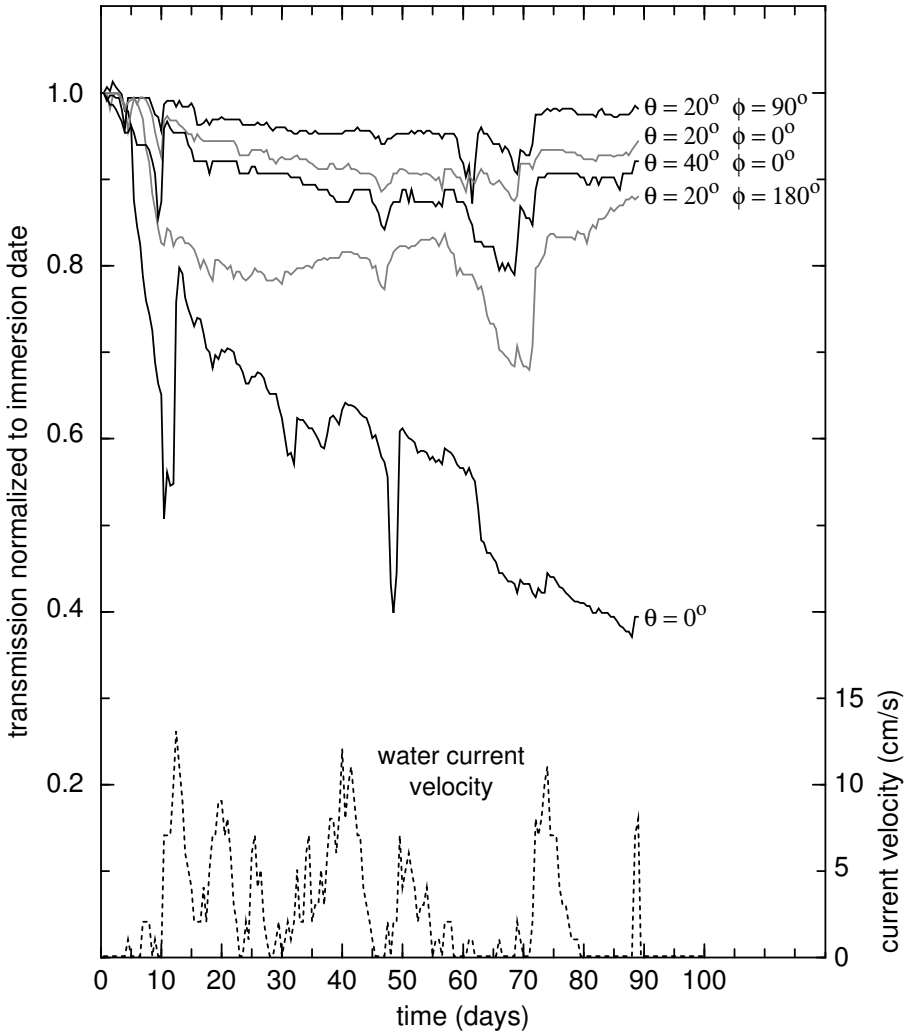

Fig. 4. Light transmission as a function of time from the first immersion, with the two spheres mounted vertically. The measurements for each of the 5 photodiodes are normalised to unity at immersion, on January 25, 1997. Curves are labeled according to the photodiode coordinates on the glass sphere surface (zenith angle θ and azimuthal angle ϕ). The current velocity is indicated at the bottom of the figure.

between the three photodiodes at zenith angle 20° indicate patchiness in the fouling.

Most important for the ANTARES detector, which will operate for several years without maintenance of the optical modules, is that there is less fouling at larger zenith angles, as confirmed with the second immersion, where photodetectors were placed at zenith angles up to 90° (figure 5). The measured loss in transmission at the equator of the sphere after 8 months is 2.7%. The fastest decrease occurs during the first few days; except for momentary fluctuations of the order of a percent, the transmission loss seems to saturate with time, with a slope of ∼0.2% per month on average. A linear extrapolation of

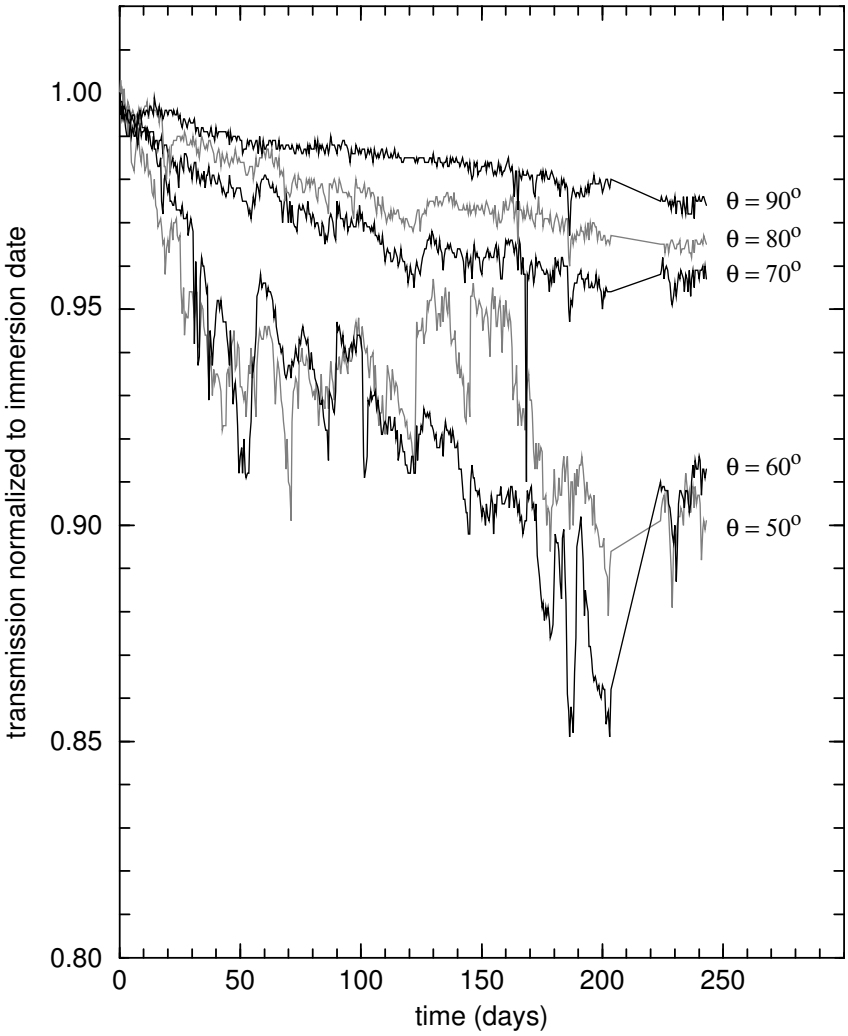

Fig. 5. Light transmission as a function of time from the second immersion, with the two spheres mounted horizontally. The measurements for each of the 5 photodiodes are normalised to unity at immersion, on July 12, 1997. Curves are labeled according to the photodiode zenith angle θ.

the 90° transmission data indicates a global loss after 1 year of ∼4%. Since this is the combination of fouling on two surfaces at 90° (the light source sphere and the detector sphere), the net loss per surface at the equator after one year is estimated to be half of the total loss, or $\sim 2\%$.

The ANTARES optical modules, consisting of photomultipliers (PMT) housed in glass spheres, will be mounted in groups of three, all PMTs with their axes oriented at 45° to the downward vertical (i.e. at zenith angles of 135°) [1]. The optically sensitive region just reaches zenith angles of 90° (equatorial). Therefore we expect the average loss in sensitivity of optical modules to be small during the several-year operation of ANTARES. A calibration system is included in the detector design to monitor the overall light collection efficiency.

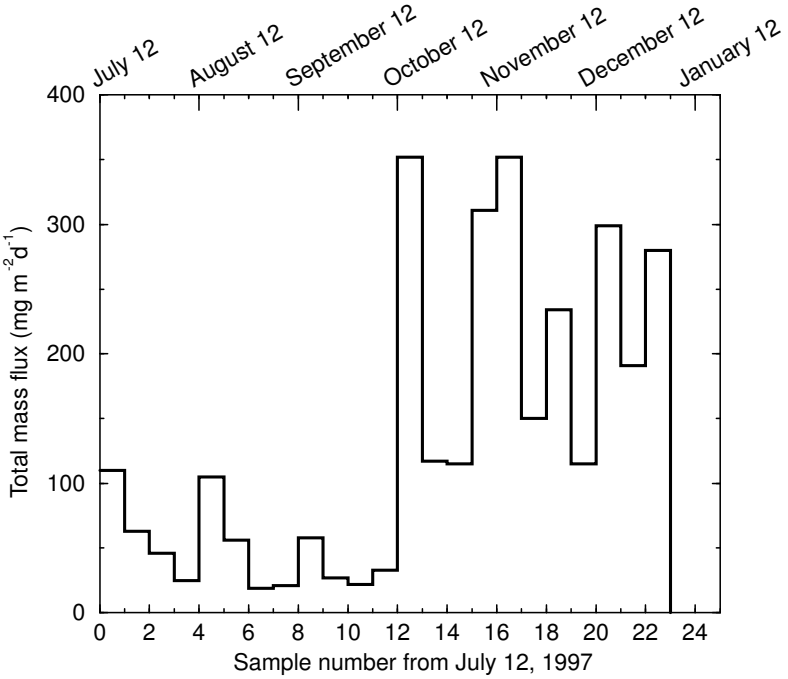

Fig. 6. Total mass fluxes at the ANTARES site over a 6-month period.

3.2 Sedimentological study

Results on variations of light transmission through optical surfaces due to fouling have been complemented by a study of core samples and measurements of the sedimentation rate.

3.2.1 Settling particles

The total mass fluxes have been measured using the sedimentation trap presented in section 2.4. They are shown in figure 6. They varied from 19 mg $\cdot$ $m^{-2} \cdot d^{-1}$ (end August) to 352 mg $\cdot m^{-2} \cdot d^{-1}$ (mid October and mid November) with a clear, apparently seasonal, jump between the two. In the summer and early autumn, low amounts of material (<100 mg $\cdot$ $m^{-2} \cdot d^{-1}$ typically) were collected. However, the mass fluxes significantly increased during the second part of the survey, in the autumn and winter periods (October to January) as has been previously observed in the Gulf of Lions (north-western Mediterranean) [6,7]. This change in the quantity of collected particles corresponded to a change in the nature of the material. The first period was mainly characterised by remains of biological production (diatoms) whereas the second period was dominated by lithogenic or detrital material (clays from the continent).

The low mass fluxes observed during the meteorologically quiet summer period

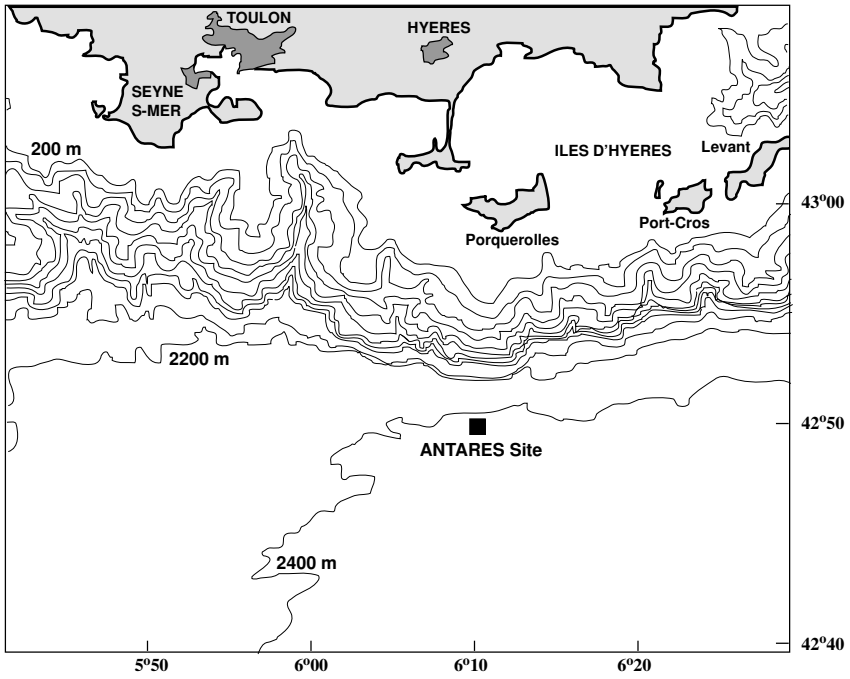

Fig. 7. Location of the ANTARES site, near the French Mediterranean coast. Contour lines indicate the depth below sea level.

can be understood from the properties of the site (see map in figure 7):

- The location is far from the Rhône river system (located ∼120 km west of Toulon) so the terrestrial influence on the ANTARES site should be limited to minor local river systems.
- The site may be affected on the surface by the Liguro-Provençal current and by its relatively high biological production. However, the samples were collected deep in the sea (> 2000 m), so significant microbial degradation of organic particles could occur during the settling time, decreasing the amount of particles reaching the sea bottom.

The high mass fluxes measured in some parts of the October to January period were probably due to the strong meteorological events typical of this season: flooding rivers and strong winds from the coast. The small Mediterranean rivers increase their liquid and solid discharges considerably during the rainy season. The location of the site, quite close to the steep continental slope (< 5 km from its base), means that it can be quickly reached by turbid flows originating from the coast during these episodes. Moreover the gusty winds can stir up the sediments on the shelf and contribute to the transfer of particles towards the abyssal plain. This explanation is consistent with the increased amount of clay in the samples collected in this period. As shown in figure 5, however, this period (90 – 180 days in figure 5) was not associated with an increase in the fouling rate.

3.2.2 Description of sediment cores

Four sediment cores have been analysed (the two remaining samples were damaged). All samples gave similar results. In this paper, we discuss the results for a single sample considered as representative of the sedimentation patterns occurring at this site on a century time scale.

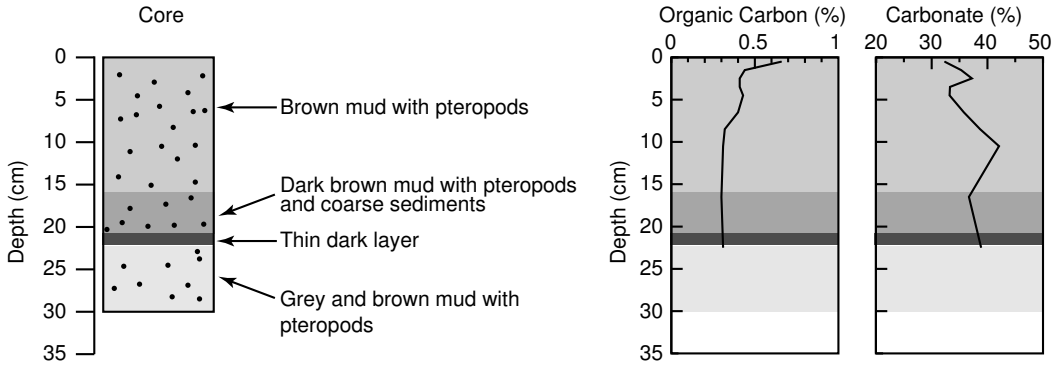

Fig. 8. Description of a core collected at the ANTARES site, with the content profiles of organic carbon and carbonates. The various shades of grey illustrate the various compositions and textures.

The sediment core shows 4 distinct sections characterised by different colours and textures (see figure 8). Starting from the upper layer, the first and longest section (0–16 cm) is mainly formed by clay sediment and biological material (pteropods), suggesting that particles produced in surface sea water strongly contributed to the sedimentation processes during the period when this layer was deposited.

The second section (16–21 cm) is dominated by coarse sediments, with a smaller fraction of biogenic particles, slowly decreasing from the top to the bottom of the section. The large detrital fraction may be interpreted as the consequence of an important resedimentation process, such as a turbidity event. This occurs when sediments located at the edge of the continental shelf become unsteady and are propelled downslope to the abyssal plain. From the sedimentation rate estimated in the following section, we can infer that the event which deposited the second layer occurred over three centuries ago.

The last two sections of the core consist of a thin dark layer on top of a substrate formed of grey and brown mud with pteropods. These two layers are over three centuries old, so they will not be discussed here.

Geochemical analyses were performed to determine water, organic carbon and carbonate contents. Total carbon contents were measured by combustion of dried samples in an analyser [5]. The organic carbon fraction was determined

[5] CS 125 from LECO, www.leco.com

on the residues remaining after treatment with 99% pure HCl to remove inorganic carbon. All inorganic carbon was assumed to be in the form of calcium carbonate ($CaCO_3$); the amount was obtained from the difference between the total carbon content and the organic carbon content. Organic carbon and carbonate rates (see figure 8) varied within the same ranges as those observed in similar deep sites in the north-western Mediterranean sea [8].

3.2.3 Sedimentation rates from ^{210}Pb radioactivity

The sedimentation rate R per unit depth (in $\mathrm{cm} \cdot \mathrm{yr}^{-1}$) on a century scale can be determined from the decay profiles of ^{210}Pb total activity as a function of depth (or time with $dz = R\,dt$), on the basis of the decay rates.

The ^{210}Pb radionucleide activity of the core was measured by high resolution alpha spectrometry [9]. Because of a small scale variability of the water content (and compaction) of the sediment, the core is cut into 1 cm-thick sections. All relevant parameters are then measured or computed for each of these centimetre-thick layers.

The ^{210}Pb radioactivity can be determined as follows:

$$A = A_{ex}(t) + A_s = \frac{F(t)}{r(t)} \exp(-\lambda t) + A_s \quad , \tag{1}$$

where A_{ex} is the excess activity due to ^{210}Pb deposited at the water-sediment interface, A_s is the ^{210}Pb activity supported by the radioactive parents present in the sediment (mostly ^{226}Ra), $\lambda = 0.03114$ yr^{-1} is the ^{210}Pb decay constant, F is the flux of ^{210}Pb delivered to the sediment (in $\mathrm{Bq} \cdot \mathrm{cm}^{-2} \cdot \mathrm{yr}^{-1}$) and r the accumulation rate per unit mass of dry sediment (in $\mathrm{g} \cdot \mathrm{cm}^{-2} \cdot \mathrm{yr}^{-1}$). The relation between r and R takes into account the compression of the sediment:

$$r = R(z) \times \rho_d \, (1 - \Phi(z)) \quad , \tag{2}$$

where $\rho_d = 2.55\ \mathrm{g} \cdot \mathrm{cm}^{-3}$ is the density of dry sediment and Φ is the porosity (percentage of the total volume of sediment that consists of pore spaces) at depth z in the core. Voids in the wet sediment being filled with water of density ρ_{water}, the porosity is determined from the water mass fraction $f_{\mathrm{water}} = 1 - m_d/m_w$ with m_w the mass of the wet sediment and m_d the mass of the dry sediment:

$$\Phi = \frac{f_{\mathrm{water}}}{f_{\mathrm{water}} + (1 - f_{\mathrm{water}}) \times \rho_{\mathrm{water}}/\rho_d} \quad . \tag{3}$$

Measures of the porosity vary between 0.56 and 0.74 for the various layers of

the core.

The model that best describes the north-western Mediterranean sea (where the ANTARES site is located) is the Constant Rate of Supply model where $F(t)$ is assumed to be constant [10].

The integrated excess ^{210}Pb activity I below the depth z of a given layer is defined as:

$$I = \int_{z}^{\infty} \rho_d \, (1 - \Phi(z')) \, A_{ex}(z') \, dz' \quad . \tag{4}$$

The accumulation rate for each layer is then obtained from:

$$r = \frac{\lambda I}{A_{ex}} \quad , \tag{5}$$

and the age of a sediment layer is given by:

$$t = \frac{1}{\lambda} \ln \frac{I_0}{I} \quad , \tag{6}$$

where I_0 is the integral over the entire sediment core.

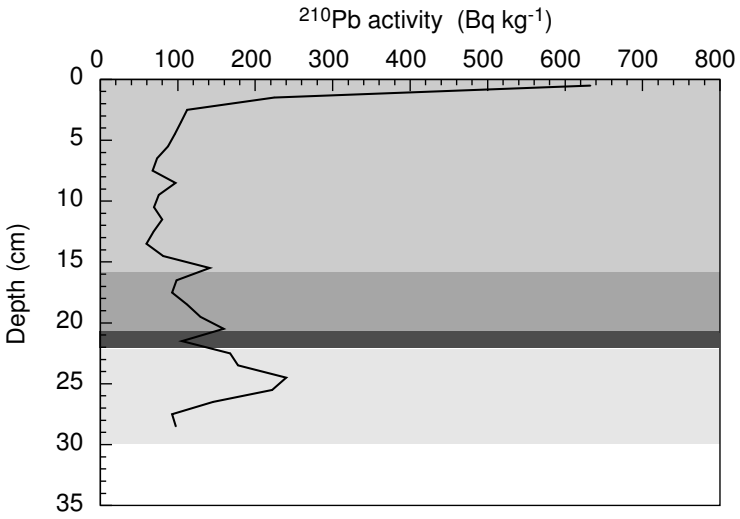

Fig. 9. ^{210}Pb raw activity profile. The shades of grey have the same meaning as in figure 8.

Figure 9 shows the ^{210}Pb activity profile, which decreases rapidly with depth. A constant contribution $A_s = 79$ Bq $\cdot$ kg^{-1} is estimated from the 7–15 cm section of the core. After correcting the ^{210}Pb activity for this background,

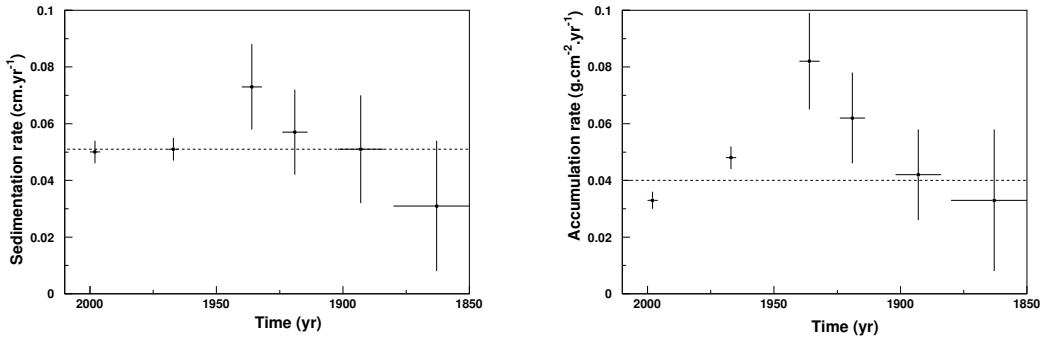

(a) Sedimentation rate R (b) Accumulation rate r

Fig. 10. Sedimentation and accumulation rates over the first 6 cm of the core (equations 2 and 5) as a function of the epoch at which the sediments deposited (equation 6). The dashed lines indicate the average rates.

the data within the first 6 cm are used to compute an average sedimentation rate $\tilde{R} = 0.052$ cm $\cdot$ yr^{-1} (see figure 10a).

The average accumulation rate $\tilde{r} = 0.040$g$\cdot$cm$^{-2}\cdot$yr^{-1} (illustrated in figure 10b) is about 8 times higher than the average total mass flux (135 mg $\cdot$ m^{-2} $\cdot$ d^{-1} or 0.005 g $\cdot$ cm^{-2} $\cdot$ yr^{-1}) determined by the trap. This discrepancy was also observed in marine environment studies. Radakovitch and Heussner suggest three possible reasons [11]:

- The accumulation rates are overestimated because of bioturbation. This process decreases the ^{210}Pb activity at the water-sediment interface by mixing the surficial sediment layer.
- The sediment trap fluxes were measured on a short period of six months whereas the average accumulation rate was determined from the first 6 cm of sediments corresponding to about 150 years. It is possible that fluxes measured over the 6-month period were lower than the average sediment accumulation rate over a century.
- Supplementary particles are delivered to the site at intermediate depths between the trap ($\sim$ 100 m above the sea bed) and the sediments. The dispersion of suspended particulate matter from the coastal region to the abyssal plain occurs through nephelometric structures that may drift along the sea bed without feeding the sediment trap.

Indeed, the accumulation rate determined above is among the highest rates found at similar depths in the North-western Mediterranean sea [12,13], which is quite surprising considering the lack of direct particle input from large rivers. This high accumulation rate may be explained by the short distance from the coast, the steep continental slope and consequent intensive processes of resuspension and transfer of particles towards the abyssal plain.

An additional core was collected under similar conditions in July 2000 for analysis of its ^{210}Pb activity profile. The excess activity is measured in the first 5 centimetres of the core and decreases rapidly from 502 $\mathrm{Bq \cdot kg^{-1}}$ at surface level to 1 $\mathrm{Bq \cdot kg^{-1}}$ between 4 and 5 centimeters, while the supported activity $A_s = 71$ $\mathrm{Bq \cdot kg^{-1}}$ is measured in the 5–11 cm section of the core. The accumulation rates r measured from the various centimetre-thick layers of the core are found to lie in the range 0.01–0.02 $\mathrm{g \cdot cm^{-2} \cdot yr^{-1}}$ and the sedimentation rates R in the range 0.03–0.02 $\mathrm{cm \cdot yr^{-1}}$, with an average of 0.022 $\mathrm{cm \cdot yr^{-1}}$ over the past century. This value is smaller than the one derived from the cores collected in December 1999 by a factor of 2, suggesting possible local variations of the sediment rates, again due to the proximity of the continental slope. These differences remain small however (of the order of a centimetre) on the scale of a century.

3.3 Water samples

The suspended particle load in water samples obtained by the Nautile in December 1998 is shown in figure 11. These data indicate that the suspended load is not constant with altitude as would have been expected if the flow of particles was purely vertical, indicating some horizontal flux as mentioned earlier. The interpretation suggested above for the high accumulation rates is supported by the high suspended particle load (2.5 $\mathrm{mg \cdot l^{-1}}$) measured in water 300 m above the bottom (and to a lesser extent close to the sea bed), which confirms the presence of nephelometric structures as vectors of impulsional and seasonal transfer.

The reservoir of settling particles, likely originating from the continental shelf or slope, represents a typical pattern of feeding deep marine basins.

3.4 Biofouling

Very little is known about bacterial adhesion on substrates in the deep sea. Studies at shallower depths have shown that a surface immersed in an aquatic environment is immediately covered with a biological slime or biofilm. The first step, occurring within minutes of immersion, is the adsorption of organic (carbohydrates, proteins, humic acids) and inorganic macromolecules already present in the environment or produced by micro-organisms [14]. These adsorbed macromolecules form the primary or conditioning film. This is an essential step since the resulting modifications of the surface properties (surface tension, surface free energy, polarity, wettability) allow subsequent adhesion of micro-organisms such as bacteria, fungi and algae. The bacterial adhesion itself occurs within a few hours after immersion. The bacterial attachment to

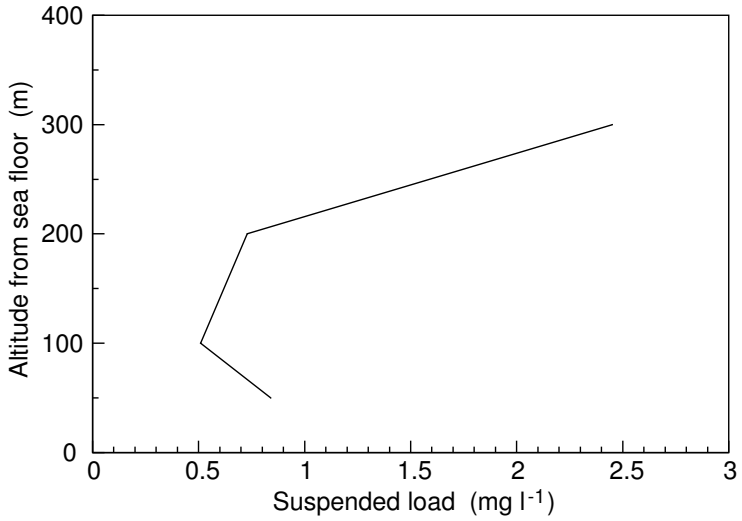

Fig. 11. Suspended load as a function of altitude from the sea floor.

the substrate is at first reversible, but later becomes irreversible because of the secretion of extracellular polymers (e.g. acidic exopolysaccharides) which develop polymeric bridging between the cell and the substrate. Once the attachment has occurred and if the physico-chemical conditions at the interface are adequate, bacteria will grow on the surface as micro-colonies. These colonies and their extracellular secretions form the biofilm. The polymers may play an important role in the loss of light transmissivity of glass spheres. The bacterial adhesion, the biofilm formation and its growth depend on different factors such as the environmental physico-chemical properties (temperature, salinity, dissolved oxygen, organic matter content, etc.), the substrate nature and micro-roughness, and the hydrodynamic conditions on the surface.

The density of bacteria after the 3-month or the 8-month exposures at the ANTARES site, obtained by epifluorescence microscopy, ranges from 10^4 to 10^6 bact$\cdot$cm^{-2} (see figure 12). Such low levels are similar to those observed on glass samples exposed for 1 to 2 weeks in shallow waters at temperatures below 15°C (the temperature measured at the ANTARES site is 13.2°C). They are explained by the low temperature and the poor quality of nutrients at these depths. Due to the very low bacterial densities, the systematic error induced by the dispersion from sample to sample masks any strong dependence with the orientation of the glass plate. There is only a weak indication that the number of bacteria after the 8-month exposure on glass plates facing upwards is larger than that observed on glass plates facing sideways or down.

Scanning electron microscopy (SEM) observations of the glass plates confirm the small total fouling (bacteria and particulates) of the surfaces. Variations with the plate orientation however is now clearly visible, as illustrated in the pictures of figure 13. While there is almost no deposit on vertical or downward facing plates, some appear on plates D and more still on plate E. The pres-

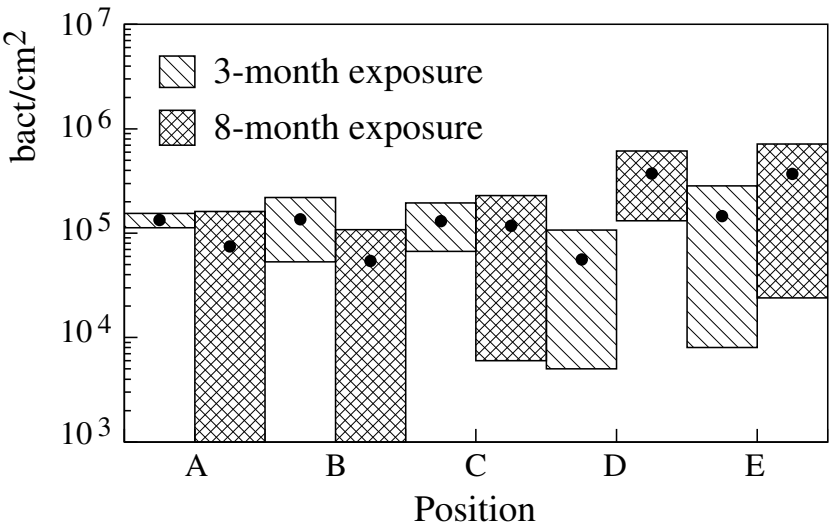

Fig. 12. The bacterial density on the glass plates, at the end of immersion, as a function of the orientation, for the 2 campaigns. Points indicate the average values and boxes illustrate the dispersion from sample to sample. Orientation labels from A (facing down) to E (facing up) are defined in Figure 3.

ence of bacteria is mostly visible on horizontal plates facing upward (E). The bacteria observed in the deep sea are smaller than those observed at shallow depths, and they seem to produce less exopolymeric material.

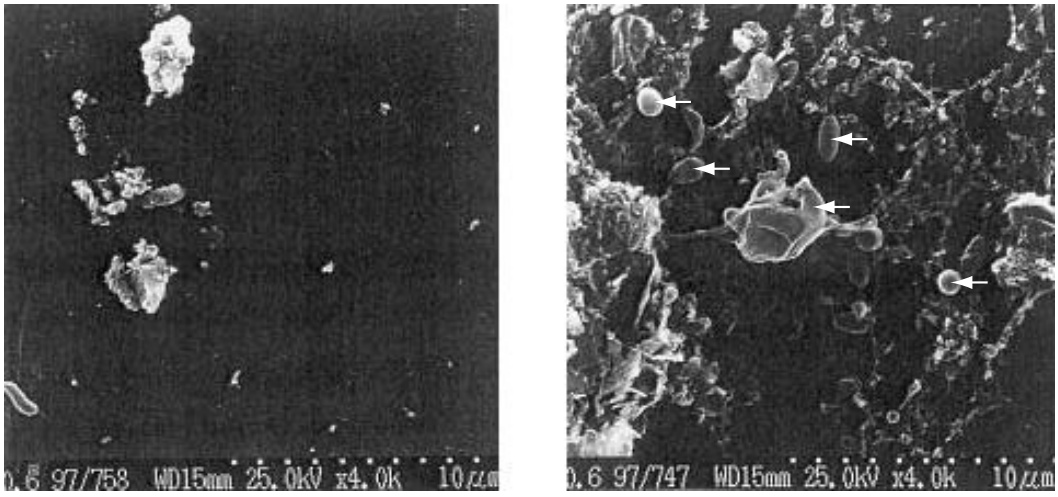

Fig. 13. Pictures obtained with the SEM. Left: on a vertical plate, right: on a horizontal plate. The small arrows in the right-hand picture show different shapes of free bacteria and bacteria embedded in exopolymers.

Light transmission through the bacterial deposits has been measured to be nearly 100% for wavelengths ranging from 350 to 850 nm [15]. The observed attenuation of light transmission should therefore be attributed to the build-up of loosely adhered particulate matter. Indeed, the SEM observations reveal high levels of particulates, especially on upward facing horizontal glass plates.

The adsorbed material is essentially made of particulates of sedimentary origin smaller than 20 μm. The washing of the sphere surface observed for currents larger than $\sim$10 cm/s points to a loose adherence of the particulates on the thin biofilm substrate. Most of the particulates were removed from the glass plates during the sampling process and transport; on the contrary, biofilm is generally very adherent and not easy to remove.

4 Conclusions

Blue light transmission through glass spheres has been measured over several months in the vicinity of the site where the ANTARES neutrino telescope will be deployed. The observed loss of transmissivity decreases steadily with increasing zenith angle. In addition, it shows a tendency to saturate with time. It reached 60% on the upper pole of a sphere after a 3-month immersion, but was found to be only 1.6% at the equator after 8 months. The loss of light transmission for a vertical glass surface is estimated to be $\sim$ 2% after one year. In order to understand the cause of the transmissivity loss, ancillary measurements of sedimentation and biofouling were performed. Despite a fairly large accumulation rate at the site, the slow growth of the transparent biofilm substrate implies a very loose adhesion of the sediments to the glass surfaces. Fouling by deposits of light-absorbing particulates is only significant for surfaces facing upwards. The ANTARES optical modules will be oriented pointing downwards, with the minimum zenith angle of the sensitive area of the PMT photocathode barely reaching the equator. Therefore, the loss of transmissivity due to the fouling is expected to be small even after several years of operation.

Analysis of the sediment core sample indicates that the most recent turbidity event in the site happened more than three centuries ago.

Acknowledgements

The authors acknowledge financial support by the funding agencies, in particular: Commissariat de l'Energie Atomique, Centre Nationale de la Recherche Scientifique, Commission Européenne (FEDER fund), Département du Var and Région Provence Alps Côte d'Azur, City of La Seyne, France; the Ministerio de Ciencia y Tecnología, Spain (FPA2000-1788); the Instituto Nazionale di Fisica Nucleare, Italy; the Russian Foundation for Basic Research, grant no. 00-15-96584, Russia; the foundation for fundamental research on matter FOM and the national scientific research organization NWO, The Netherlands; the Particle Physics and Astronomy Research Council, United Kingdom.

References

[1] http://antares.in2p3.fr

[2] ANTARES Collaboration, Nucl. Phys. Proc.Suppl. **100** (2001) 341-343 and publications listed in [1]

[3] P. Amram et al., ANTARES Collaboration, Astroparticle Physics **13** (2000) 127-136

[4] http://www.ifremer.fr/fleet/systemes_sm/engins/nautile.htm

[5] S. Heussner et al., Continental Shelf Research **10** (1990) 943

[6] A. Monaco et al., Continental Shelf Research **10** (1990) 959

[7] A. Monaco et al., Deep Sea Research I **46** (1999) 1483

[8] R. Buscail et al., Continental Shelf Research **10** (1990) 1089

[9] A. Abassi, (unpublished) PhD thesis Université de Perpignan (1998)

[10] P.G. Appleby and F. Oldfield, Catena **5** (1978) 1

[11] O. Radakovitch and S. Heussner, Deep Sea Research II **46** (1999) 2175-2203

[12] Z. Zuo et al., Oceanologica Acta **14** (1991) 3

[13] O. Radakovitch, (unpublished) PhD thesis Université de Perpignan (1995)

[14] C. Compère et al., Biofouling **17(2)** (2001) 129-145

[15] BROS: Biofouling Reduction on Optical Systems, Final Report, Task 8, Bacterial and Algal Accumulation on Optical Surfaces, MAS3-CT95-028/B3 (1998)